Coupling between an Abruptly Terminated Optical Fiber and a Dielectric Planar Waveguide

CHRISTOS N. CAPSALIS AND NIKOLAOS K. UZUNOGLU, MEMBER, IEEE

Abstract — **The coupling between an optical fiber and a dielectric planar waveguide is analyzed when both guides are terminated abruptly and are facing each other. Mixed spectrum eigenwave representations of fields are employed inside the waveguides while Fourier integrals are utilized to describe the field in the space between the two guides. A coupled system of integral equations is derived by satisfying the boundary conditions on the terminal planes of both waveguides. A weak guidance approximation is assumed to facilitate the analysis. Numerical results are presented for several coupling geometries. Misalignment losses and coupling optimization phenomena are investigated.**

I. Introduction

A PROBLEM OF great importance in optical communication systems is to transfer light energy from a planar or a linear waveguide to a single-mode optical fiber, or vice versa. The planar waveguide could be an injection laser or a semiconductor detector. Recently, composite packages utilizing cylindrical microlenses have been tried as a means of improving the coupling efficiency of laser emission into optical fibers [1], [2], [3]. However these techniques are still under investigation and as yet no standard coupling method has emerged. The alignment of microlenses is expected to be a problem. The laser active layer thickness is around 0.2 μm while the single-mode fiber core diameter is approximately 8 μm. Therefore, in principle, the emitted radiation from a semiconductor laser can be coupled into an optical fiber if the distance between them is sufficiently small. Then it is crucial to examine the achievable coupling efficiencies and the misalignment tolerances of this simple coupling scheme. The positioning of the fiber in front of the planar waveguide can be done by using mechanical means, epoxy resin fixing, or even monolithic integration techniques.

Theoretical analyses of laser diode to multimode fiber coupling have been undertaken by several researchers [3]–[6] when cylindrical or spherical lenses are employed. Usually ray-tracing techniques are applied to estimate the coupling efficiencies.

Manuscript received April 20, 1987; revised July 15, 1987.

The authors are with the Department of Electrical Engineering, National Technical University of Athens, Athens, 106 82 Greece.

IEEE Log Number 8716918.

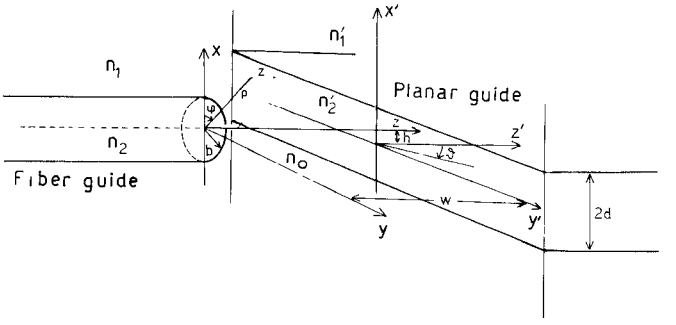

Fig. 1. Single-mode fiber to planar waveguide coupling geometry.

The present paper deals with the coupling of an abruptly terminated dielectric slab waveguide with a single-mode fiber. In Fig. 1 the coupling geometry is defined. A single-mode fiber of radius b is facing a planar waveguide of $2d$ guiding layer thickness. The core and cladding region refractive indices of the fiber guide are designated n_2 and n_1, respectively. The corresponding guiding layer and cover-substrate refractive indices of the planar waveguide are denoted by n_2' and n_1', respectively. The space between the two guides is assumed to be homogeneous and its refractive index is denoted by n_0. The distance between the abruptly terminated guide parallel terminal planes is w. The planar waveguide is taken to be of infinite width along the y axis. The displacement of the propagation axes of the two guides along the x axis is denoted by h.

In the following analysis, an $\exp(+j\omega t)$ time variation is assumed for the field quantities and is suppressed throughout the analysis. The free-space wavenumber is $k_0 = \omega/c$, where c is the velocity of light in vacuum.

II. Analysis of the Coupling Problem

In treating the coupling between a planar and a single-mode fiber waveguide, an analytical technique bearing similarities with a method developed in analyzing abruptly terminated dielectric slab waveguides [7] will be utilized. The method to be presented relies on the use of mixed spectral field representations inside the guiding regions, while a Fourier integral representation is employed in the intermediate space between the two waveguides.

0018-9480/87/1100-1043$01.00 ©1987 IEEE

In the following analysis, an incident guided wave propagating inside the fiber along the positive z axis (see Fig. 1) is assumed. Then the dominant mode amplitudes are computed inside the planar waveguide. Although in practice usually the laser diodes are used to feed power into fibers, because of the reciprocity principle, the analysis of the opposite problem presented in this paper provides the anwer to the practical problem of laser diode–fiber coupling.

The single-mode fiber can support two degenerate HE_{11} modes. In optical guides the weak guidance condition always is satisfied [8]. This means that the validity of $n_2 \gtrsim n_1$ and $n_2' \gtrsim n_1'$ could be used to simplify considerably the field expressions and description of guided waves in either fiber or planar waveguides. Then the guided waves in fiber waveguide are linearly polarized. In the case of a single-mode fiber, there are two orthogonal modes polarized linearly along the x and y axes, respectively. Then a single transversal electric field component, E_x or E_y, could be used to describe the propagation of guided waves. The gain-guided laser diodes operate exclusively with the dominant TE (transverse electric) mode. Therefore, inside the planar guide the dominant electric field component will be along the y axis (see Fig. 1). It is therefore of interest to examine mainly the case when the incident wave from the fiber waveguide is polarized parallel to the y axis. In addition to guided modes, the presence of longitudinal discontinuities along the propagation axes on both waveguides implies the excitation of radiation modes. The mixed eigenwave spectrum used in the following consists of the guided modes (discrete spectrum) plus the radiation modes (continuous spectrum). The nondepolarizing nature of the encountered discontinuities allows the use of a single field component in describing the radiation modes [9]. Then it is possible to express the radiation modes in terms of the electric field y component. Therefore a scalar wave $\Psi(\boldsymbol{r})$ could be used to describe the field either inside the fiber or planar waveguide.

A. Field Expansion inside the Fiber

In describing the field distribution inside the fiber waveguide ($z < 0$, see Fig. 1) a mixed spectrum of eigenwaves is constructed by determining the solution of the wave equation

$$\left(\nabla^2 + k_0^2 n_i\right)\Psi(\rho, \varphi, z) = 0 \qquad \text{for } i = 1,2 \tag{1a}$$

in cylindrical coordinates ρ, φ, z, defined in Fig. 1, subject to the boundary conditions

$$\Psi(\rho, \varphi, z)\big|_{\rho = b-} = \Psi(\rho, \varphi, z)\big|_{\rho = b+} \tag{1b}$$

$$\left.\frac{\partial \Psi(\rho, \varphi, z)}{\partial \rho}\right|_{\rho = b-} = \left.\frac{\partial \Psi(\rho, \varphi, z)}{\partial \rho}\right|_{\rho = b+} \tag{1c}$$

on the core–cladding $\rho = b$ interface. Equations (1a)–(1c) are valid only for weakly guiding fibers, and their approximate nature should be stressed. In the Appendix the mixed spectrum of a weakly guiding fiber is given. Then the Ψ_f electric field (polarized along the y axis) inside the single-mode fiber ($z < 0$, see Fig. 1) can be expanded as follows:

$$\Psi_f(\rho, \varphi, z) = \psi_0(\rho, \varphi)\left(e^{-j\beta_0 z} + R_0 e^{j\beta_0 z}\right) + \int_0^{+\infty} q\,dq \sum_{m=-\infty}^{+\infty} R_m(q)\psi_m(\rho, \varphi|q)e^{j\beta z} \tag{2}$$

where $\psi_0(\rho, \varphi)$ is the guided-mode field distribution on a $z =$ constant transversal plane and $\psi_m(\rho, \varphi|q)$ is the corresponding radiation-mode field. Furthermore β_0 and $\beta = (k_0^2 n_i^2 - q^2)^{1/2}$ are the propagation constants of the guided and radiation modes, respectively. The unknown terms R_0 and $R_m(q)$ in (2) are the reflection coefficients of the guided and radiation modes, respectively.

B. Field Expansion inside the Planar Guide

The three-dimensional nature of the fiber guide radiation pattern excludes the possibility of having y-axis-independent-type waves inside the planar guide, the type most frequently analyzed in the literature [10]. Then it is obvious that only hybrid modes (i.e., combination of transverse electric and magnetic waves) should be excited inside the planar waveguide. Indeed, if a rigorous solution is desired, hybrid-mode field expressions should be adopted in expanding the field. However because of the weak guidance condition, in a similar way to the fiber guide, an approximate linearly polarized field distribution could be taken to simplify the analysis. This assumption ensures tractability, and its validity can be checked by observing the variation of the obtained solution along the y axis, which should be slow [11]. To this end, the Ψ_p-dominant y-polarized electric field inside the planar guide can be written as follows:

$$\Psi_p(x', y', z') = \int_{-\infty}^{+\infty} da \sum_{s=e,o} \left\{ \sum_{n=1}^{N_s} A_{sn}(a) e^{-jv_{sn}z'} U_{sn}(x') + \int_0^{+\infty} dp\, B_s(a, p) e^{-j\beta_1 z'} \varphi_s(x', p) \right\} e^{-jay'} \tag{3}$$

where the subscripts $s = e$ and o are to show that the even and odd modes; (x', y', z') are the local Cartesian coordinates of the planar guide (see Fig. 1) and are connected to the fiber coordinates with the relations

$$\begin{aligned} x' &= y - h \\ y' &= y \\ z' &= z - w. \end{aligned} \tag{4}$$

In (3) the set of functions $\{U_{S1}(x'), U_{S2}(x'), \cdots, U_{S_{N_s}}(x')\}$ is the discrete part of the spectrum. N_e and N_o are the number of even and odd symmetry guided modes, respectively. The radiation modes, constituting the continuous spectrum, are described with the $\varphi_s(x', p)$ functions. Notice that only waves propagating along the positive z axis are taken into account in (3). The mode functions $U_{sn}(x)$ and $\varphi_s(x, p)$ and their basic properties are given in the Appendix. The dependence on the $y' = y$ variable is described with the $\exp(-jay)$ Fourier term. The values of v_{sn} and the guided- and radiation-mode propagation constants, depending on the value of a, are determined by solving the transcendental equations given in the Appendix. Finally, $A_{sn}(a)$ and $B_s(a, p)$ are unknown coefficients to be determined.

C. Field Description in the Space between the Two Guides

Assuming in this region also the validity of the single-component electric field approximation and using cylindrical wave functions, the following expansion is obtained:

$$\Psi_a(\rho, \varphi, z) = \int_0^{\infty} \lambda\, d\lambda \sum_{m=-\infty}^{+\infty} J_m(\lambda\rho) e^{jm\varphi} \cdot \left(C_m(\lambda) e^{-j\tau z} + C'_m(\lambda) e^{j\tau z}\right) \quad (5)$$

where $\tau = (k_0^2 n_0^2 - \lambda^2)^{1/2}$, $J_m(x)$ is the mth-order Bessel function, and C_m, C'_m are unknown expansion coefficients to be determined.

D. Boundary Conditions

In order to determine the unknown coefficients appearing in (2), (3), and (5), the boundary conditions on the $z = 0$ and $z = w$ interface planes should be satisfied. An integral equation approach will be employed in terms of the unknown electric field distributions $\mathscr{E}_1(\rho, \varphi)$ and $\mathscr{E}_2(x, y)$ on the $z = 0$ and $z = w$ planes, respectively. By employing the orthogonality relations of the $\{\psi_m(\rho, \varphi), \psi_m(\rho, \varphi|q), m = 0, \pm 1, \cdots, 0 < q < +\infty\}$ fiber mixed spectrum eigenwaves, given in the Appendix, the unknown coefficients $R_0, R_m(q)$ of (2) can be written as follows:

$$R_0 = -1 + \frac{1}{2\pi} \int_0^{2\pi} d\varphi \int_0^{+\infty} \rho\, d\rho\, \mathscr{E}_1(\rho, \varphi) \psi_0^*(\rho, \varphi) \quad (6)$$

$$R_m(q) = \frac{1}{2\pi} \int_0^{2\pi} d\varphi \int_0^{+\infty} \rho\, d\rho\, \mathscr{E}_1(\rho, \varphi) \psi_m^*(\rho, \varphi|q). \quad (7)$$

Applying similar considerations by using the planar waveguide mixed spectrum eigenwaves (see the Appendix), the unknown coefficients in (3) are found to be

$$A_{sn}(a) = \frac{1}{2\pi} \int_{-\infty}^{+\infty} dy' \int_{-\infty}^{+\infty} dx'\, \mathscr{E}_2(x', y') e^{jay'} U_{sn}(x') \quad (8)$$

$$B_s(a, p) = \frac{1}{2\pi} \int_{-\infty}^{+\infty} dy' \int_{-\infty}^{+\infty} dx'\, \mathscr{E}_2(x', y') e^{jay'} \varphi_s(x', p). \quad (9)$$

In order to express the unknown coefficients $C_m(\lambda)$ and $C'_m(\lambda)$ of (5) in terms of the $\mathscr{E}_1(\rho, \varphi)$ and $\mathscr{E}_2(x, y)$ field distributions, use is made of the orthogonality relations,

$$\int_0^{+\infty} \rho\, d\rho\, J_m(\lambda, \rho) J_m(\lambda', \rho) = \frac{1}{\lambda} \delta(\lambda - \lambda') \quad (10)$$

$$\frac{1}{2\pi} \int_0^{2\pi} d\varphi\, e^{j(m-m')\varphi} = \delta_{mm'}. \quad (11)$$

Then it can easily be shown that

$$C_m(\lambda) + C'_m(\lambda) = \frac{1}{2\pi} \int_0^{2\pi} d\varphi \int_0^{+\infty} \rho\, d\rho\, J_m(\lambda, \rho) e^{-jm\varphi} \mathscr{E}_1(\rho, \varphi) \quad (12)$$

$$C_m(\lambda) e^{-j\tau w} + C'_m(\lambda) e^{j\tau w} = \frac{1}{2\pi} \int_0^{2\pi} d\varphi \int_0^{\infty} \rho\, d\rho\, J_m(\lambda, \rho) e^{-jm\varphi} \mathscr{E}_2(x', y') \quad (13)$$

where the continuity of the electric field on the $z = 0$ and $z = w$ planes is also incorporated.

In addition to the electric field, the continuity of the tangential magnetic field components on the $z = 0$ and $z = w$ planes should be satisfied. Then it is required to have

$$\frac{\partial \Psi_f}{\partial z} = \frac{\partial \Psi_a}{\partial z} \qquad \text{at } z = 0 \quad (14)$$

and

$$\frac{\partial \Psi_a}{\partial z} = \frac{\partial \Psi_p}{\partial z} \qquad \text{at } z = w. \quad (15)$$

On substituting (2), (3), and (5) into the continuity conditions (14), and (15) and then introducing the expressions (6)–(9), (12), and (13), the following system of integral

equations is obtained:

$$-\beta_0\Psi_0(\rho,\varphi)+\beta_0\left(\frac{1}{2\pi}\int_0^{2\pi}d\varphi'\int_0^{+\infty}\rho'\,d\rho'\,\mathscr{E}_1(\rho',\varphi')\Psi_0(\rho',\varphi')-1\right)\Psi_0(\rho,\varphi)$$

$$+\frac{1}{2\pi}\int_0^{+\infty}q\,dq\sum_{m=-\infty}^{+\infty}\beta\int_0^{2\pi}d\varphi'\int_0^{+\infty}\rho'\,d\rho'\,\mathscr{E}_1(\rho',\varphi')\Psi_m(\rho',\varphi'|q)\Psi_m(\rho,\varphi|q)$$

$$=\int_0^{+\infty}\lambda\,d\lambda\sum_{m=-\infty}^{+\infty}J_m(\lambda\rho)e^{jm\varphi}\tau\frac{1}{2\pi}$$

$$\cdot\left[-\frac{1}{1-e^{-j2\tau w}}\int_0^{2\pi}d\varphi'\int_0^{+\infty}\rho'\,d\rho'\,J_m(\lambda,\rho')e^{-jm\varphi'}\mathscr{E}_1(\rho',\varphi')-e^{-j\tau w}\mathscr{E}_2(x',y')\right)$$

$$+\frac{1}{1-e^{j2\tau w}}\int_0^{2\pi}d\varphi'\int_0^{+\infty}\rho'\,d\rho'\,J_m(\lambda\rho')e^{-jm\varphi'}\left(\mathscr{E}_1(\rho',\varphi')-e^{j\tau w}\mathscr{E}_2(x',y')\right]$$

$$\int_0^{+\infty}\lambda\,d\lambda\sum_{m=-\infty}^{+\infty}J_m(\lambda\rho)e^{jm\varphi}\tau\left[-\frac{e^{-j\tau w}}{1-e^{-2j\tau w}}\int_0^{2\pi}d\varphi'\int_0^{+\infty}\rho'\,d\rho'\,J_m(\lambda\rho')e^{-jm\varphi'}\right.$$

$$\left.\cdot\left(\mathscr{E}_1(\rho',\varphi')-e^{-j\tau w}\mathscr{E}_2(x',y')\right)+\frac{e^{j\tau w}}{1-e^{j2\tau w}}\int_0^{2\pi}d\varphi'\int_0^{+\infty}\rho'\,d\rho'\,J_m(\lambda\rho')e^{-jm\varphi'}\right] \tag{16}$$

$$\left(\mathscr{E}_1(\rho',\varphi')-e^{j\tau w}\mathscr{E}_2(x',y')\right)=-\int_{-\infty}^{+\infty}da\sum_{s=e,0}\sum_{n=1}^{N_s}\int_{-\infty}^{+\infty}dy'\int_{-\infty}^{+\infty}dx'$$

$$\cdot\mathscr{E}_2(x',y')e^{jay'}U_{sn}(x')v_{sn}e^{-jay}U_{sn}(x)-\int_{-\infty}^{+\infty}da\int_0^{+\infty}dp\sum_{s=e,0}\int_{-\infty}^{+\infty}dy'\int_{-\infty}^{+\infty}dx'$$

$$\cdot\mathscr{E}_2(x',y')e^{jay'}\varphi_s(x',p)\beta_1e^{-jay}\varphi_s(x,p). \tag{17}$$

The system of equations in (16) and (17) constitutes a Fredholm integral equation of the first kind. In general it is preferable to work with Fredholm integral equations of the second kind, which are amenable to iterative or approximate solutions. Furthermore examining the physical aspects of the coupling geometry, it is observed that when $n_1=n_2$ and $n_1'=n_2'$, a simple boundary value problem is encountered. Therefore, since $n_1\sim n_2$ and $n_1'\sim n_2'$ is always satisfied, it is desirable to transform the system (16) and (17) into a Fredholm system of equations of the second kind. The homogeneous term of this system should be identical with the field distributions $\mathscr{E}_1(\rho,\varphi)$ and $\mathscr{E}_2(x',y')$ obtained when the reflection from a dielectric slab between two different media is solved by simple analytical techniques [12]. Furthermore, when $n_1=n_2$ and $n_1'=n_2'$, the contributions from the integrations should vanish. Then following similar analytical techniques described in [7] in treating the diffraction from an abruptly terminated dielectric slab waveguide, after lengthy algebra the following system is obtained:

$$\mathscr{E}_1(\rho,\varphi)=\mathscr{E}_{10}(\rho,\varphi)$$

$$+\int_0^{2\pi}d\varphi'\int_0^{+\infty}\rho'\,d\rho'\left(K_{11}(\rho,\varphi|\rho',\varphi')\mathscr{E}_1(\rho',\varphi')\right.$$

$$\left.+K_{12}(\rho,\varphi|\rho',\varphi')\mathscr{E}_2(\rho',\varphi')\right) \tag{18}$$

$$\mathscr{E}_2(\rho,\varphi)=\mathscr{E}_{20}(\rho,\varphi)$$

$$+\int_0^{2\pi}d\varphi'\int_0^{+\infty}\rho'\,d\rho'\left(K_{21}(\rho,\varphi|\rho',\varphi')\mathscr{E}_1(\rho',\varphi')\right.$$

$$\left.+K_{22}(\rho,\varphi|\rho',\varphi')\mathscr{E}_2(\rho',\varphi')\right) \tag{19}$$

where

$$\mathscr{E}_{11}(\rho,\varphi)=\frac{2\left(\frac{\beta_0}{k_0n_0}\psi_0(\rho,\varphi)-\frac{e^{jk_0n_0w}}{1-e^{2jk_0n_0w}}\mathscr{E}_2(\rho,\varphi)\right)}{n_2+\frac{1+e^{j2k_0n_0w}}{e^{j2k_0n_0w}-1}} \tag{20}$$

$$\mathscr{E}_{20}(\rho,\varphi)=\frac{\mathscr{E}_1(\rho,\varphi)2e^{jk_0n_0w}}{\left(-n_1'+\frac{1+e^{2jk_0n_0w}}{1-e^{2jk_0n_0w}}\right)(1-e^{2jk_0n_0w})} \tag{21}$$

and solving for $\mathscr{E}_1$ and $\mathscr{E}_2$. Then, substituting this solution into the right-hand sides of (18) and (19), the first-order solution is derived. The use of orthogonality relations given in the Appendix and the integration formulas for the products of two Bessel functions resulted in analytic expressions except for the cross products involving fiber and planar guide eigenwaves. The latter integrals are computed numerically. The exceptionally lengthy formulas and the little practical interest in knowing directly the $\mathscr{E}_1$ and $\mathscr{E}_2$ field distributions restrained us from giving their expressions. Instead of this, the reflection coefficient R_0 and the coupling coefficient computed form the $A_{e1}(\alpha)$ term are quoted in the next section.

$$K_{11}(\rho,\varphi|\rho',\varphi')=-\frac{1}{2\pi}(\beta_0-k_0n_2)\psi_0(\rho,\varphi)\psi_0^*(\rho',\varphi')+\sum_{m=-\infty}^{+\infty}\int_0^{+\infty}q\,dq\,(\beta-k_0n_2)\psi_m^*(\rho,\varphi)\psi_m(\rho',\varphi')$$
$$+\int_0^{+\infty}\lambda\,d\lambda\left[\frac{\tau(1+e^{2j\tau w})}{e^{2j\tau w}-1}-\frac{(1+e^{2jk_0n_0w})}{e^{j2k_0w}-1}\right]\sum_{m=-\infty}^{+\infty}J_m(\lambda\rho)J_m(\lambda\rho')e^{jm\varphi}e^{-jm\varphi'} \tag{22}$$

$$K_{12}(\rho,\varphi|\rho',\varphi')=\frac{1}{\pi}\int_0^{+\infty}\lambda\,d\lambda\left[-\frac{\tau e^{j\tau w}}{1-e^{2j\tau w}}+\frac{k_0n_0e^{jk_0n_0w}}{1-e^{2J_0k_0n_0w}}\right]\sum_{m=-\infty}^{+\infty}J_m(\lambda\rho)J_m(\lambda\rho')e^{jm\varphi}e^{-jm\varphi'} \tag{23}$$

$$K_{21}(\rho,\varphi|\rho',\varphi')=\frac{1}{\pi}\int_0^{+\infty}\lambda\,d\lambda\left[\frac{\tau e^{j\tau w}}{1-e^{2j\tau w}}-\frac{k_0n_0e^{jk_0n_0w}}{1-e^{2jk_0n_0w}}\right]\sum_{m=-\infty}^{+\infty}J_m(\lambda\rho)J_m(\lambda\rho')e^{jm\varphi}e^{-jm\varphi'} \tag{24}$$

$$K_{22}(\rho,\varphi|\rho',\varphi')=-\frac{1}{\pi}\int_0^{+\infty}\lambda\,d\lambda\left[\frac{\tau(1+e^{j2\tau w})}{1-e^{2j\tau w}}-\frac{k_0(1+e^{2jk_0n_0w})}{1-e^{2jk_0n_0w}}\right]\sum_{=-\infty}^{+\infty}J_m(\lambda\rho)J_m(\lambda\rho')e^{jm\varphi}e^{-jm\varphi'}$$
$$+\frac{1}{2\pi}\int_{-\infty}^{+\infty}da\,e^{-ja(y-y')}\sum_{s=e,o}\sum_{n=1}^{N_s}(v_{sn}-k_0n_1')U_{sn}(x)U_{sn}(x')+\int_0^{+\infty}dp\,\varphi_s(x,p)\varphi_s(x',p)(\beta_1-k_0n_1'). \tag{25}$$

Notice that in (25) the transformations $x=\rho\cos\varphi$, $x'=\rho'\cos\varphi'$ and $y=\rho\sin\varphi$, $y'=\rho'\sin\varphi'$ should be incorporated.

It can easily be shown that if $n_1\to n_2$ and $n_1'\to n_2'$, then $K_{ij}\to 0$ $(i=1,2;\ j=1,2)$ and the solution of (19), (20) reduces to the elementary problem of reflection from a dielectric layer placed between two different media. Therefore, following exactly the same raison d'être as in [7], an iterative procedure could be used to solve approximately the system (18) and (19). In this paper up to first-order iterative solutions have been obtained. The zeroth-order solution is obtained by setting

$$\mathscr{E}_1(\rho,\varphi)=\mathscr{E}_{10}(\rho,\varphi)$$
$$\mathscr{E}_2(\rho,\varphi)=\mathscr{E}_{20}(\rho,\varphi) \tag{26}$$

III. Computation of Coupling and Reflection Coefficients

Assuming the $\mathscr{E}_1(\rho,\varphi)$ and $\mathscr{E}_2(x',y')$ fields are known on the $z=0$ and $z=w$ interface planes, it is possible to compute the electric fields in either $z<0$ or $z>w$ semi-infinite spaces. To this end, the first-order iterative solutions $\mathscr{E}_1$, $\mathscr{E}_2$ are substituted into (6) and (8) to derive the guided wave amplitudes inside the fiber and planar waveguides, respectively. The use of the first-order approximation is justified from the conclusions of the analysis of the abruptly terminated planar dielectric waveguide [7], where a satisfactory convergence has been observed. The use of orthogonality relations given in the Appendix and integrals for the product of Bessel functions resulted in the following expression from the reflection coefficient on the fiber guide:

$$R_0=-1+B_1(w)\left[2\beta_0\left(1-A_2(w)\frac{4n_0e^{jk_0n_0w}}{1-e^{2jk_0n_0w}}\right)-(\beta_0-k_0n_2)\frac{2\beta_0}{k_0n_0}A_1(w)\right]$$
$$-\frac{2\beta_0}{k_0n_0}B_1(w)\int_0^{+\infty}\lambda\,d\lambda\left[(C_1(\lambda,w)-C_2(w)A_1(w)-4A_2(w)(C_3(\lambda,w)-C_4(w))\right] \tag{27}$$

where

$$A_1(w)=\frac{(n_0-n_1')+e^{jk_0n_0w}(n_0+n_1')}{(n_0-n_1')(n_2-n_0)+e^{2jk_0n_0w}(n_0+n_1')(n_0+n_2)} \tag{28}$$

$$A_2(w)=\frac{e^{jk_0n_0w}}{(n_0-n_1')(n_2-n_0)+e^{j2k_0n_0w}(n_0+n_1')(n_0+n_2)} \tag{29}$$

$$B_1(w)=\frac{e^{j2k_0n_0w}-1}{k_0n_2(e^{2jk_0n_0w}-1)+k_0n_0(1+e^{2jk_0n_0w})} \tag{30}$$

$$C_1(\lambda,w)=\frac{\tau(1+e^{2j\tau w})}{e^{2j\tau w}-1} \qquad C_2(w)=C_1(0,w) \tag{31}$$

$$C_3(\lambda,w)=\frac{\tau e^{j\tau w}}{e^{j2\tau w}-1} \qquad C_4(w)=C_3(0,w). \tag{32}$$

In a similar way, the amplitude coefficient of the dominant-systemtric even TE mode propagating inside the planar waveguide is obtained as

$$\begin{aligned}A_{e1}(a)=\frac{2\beta_0}{\pi}&\left[\int_{-\infty}^{+\infty}dy\int_{-\infty}^{+\infty}dx'e^{jay}U_{e1}(x')\Psi_0(\rho,\varphi)\right]\\&\left[B_2(w)A_1(w)\frac{e^{jk_0w}}{1-e^{2jk_0w}}+\frac{A_2(w)}{k_0n_0}(v_{e1}-k_0n_1)\right]\\&-B_2(w)\frac{4\beta_0C_0}{k_0n_0}\int_a^{+\infty}\lambda\,d\lambda\,[A_1(w)(C_3(\lambda,w)\\&-C_4(w))-A_2(w)(C_1(\lambda,w)-C_2(w))]\\&\cdot I_u(\lambda)\frac{k_0^2(n_2^2-n_1^2)b}{(a_0^2-\lambda^2)(\gamma^2+\lambda^2)}(\gamma K_1(\gamma b)J_0(\lambda b)\\&-\lambda K_0(\gamma b)J_1(\lambda b))\end{aligned} \tag{33}$$

where C_0, a_0, γ, and $I_u(\lambda)$ are given in the Appendix. In computing the numerical values of the $A_{e1}(a)$ coefficients, a two-dimensional numerical integration is performed involving the product of the $U_{e1}(x)$ and $\Psi_0(\rho,\varphi)$ mode functions. Owing to the highly spatial concentration of these functions near the guiding axes, no convergence problems are encountered. Furthermore, it is necessary to compute in both the R_0 and $A_{e1}(a)$ coefficients improper integrals with respect to the λ integration variable. To this end, a 12-point Gaussian quarature numerical integration procedure is employed after dividing the integration domains into an adequate number of subintervals. The truncation of the infinite bounds is taken sufficiently high to ensure convergence.

IV. Numerical Results

Numerical computations have been performed by using the analytical results obtained in the previous sections. In all the computations, the free-space radiation wavelength is taken to be

$$\lambda_0=1.55\ \mu\text{m}\ (=2\pi/k_0).$$

The single-mode fiber characteristics are

$$b=5\ \mu\text{m} \qquad n_1=1.450 \qquad n_2=1.454$$

and the corresponding planar guide dimensions modeling a GaAs laser diode are taken to be

$$d=0.5\ \mu\text{m} \qquad n_1'=3.40 \qquad n_2'=3.61.$$

The space between the two guides is taken to be air, i.e., $n_0=1$. In order to compute the coupling efficiency, the following mode power ratio is defined:

$$\text{Coupling Efficiency} = CE = \frac{\left\{\begin{array}{l}\text{planar guide dominant TE}_0\text{ mode}\\ \text{total power}\ (-\infty<a<+\infty)\end{array}\right\}}{\text{incident fiber mode power}}. \tag{34}$$

On substituting the planar guide dominant-mode function into the Poynting theorem written on the $z=w$ plane, the total power coupled into the planar guide is found to be

$$P_p=\frac{1}{120k_0}\int_{-\infty}^{+\infty}da\,|A_{e1}(a)|^2v_{e1}(a). \tag{35}$$

In a similar way, the incident fiber mode total power is

$$P_f=\frac{n_1}{120} \tag{36}$$

when the $\int_{-\infty}^{+\infty}\rho\,d\rho\,|\Psi_0(\rho,\varphi)|^2=1$ normalization condition is satisfied. Then, according to (34),

$$CE=\frac{P_p}{P_f}=\int_{-\infty}^{+\infty}da\,|A_{e1}(a)|^2\frac{v_{e1}(a)}{k_0n_1}. \tag{37}$$

Notice that in integrating the Poynting vector on the $z=w$ plane the total power coupled into the TE planar guide is obtained as a superposition of $|A_{e1}(a)|^2$ mode amplitudes. A Simpson rule numerical integration procedure is employed to compute the integral in (37). For a given specific value of a, the guided wave inside the planar guide travels parallel to the unit vector.

$$\hat{N}_a=\hat{z}'\cos\theta+\hat{y}'\sin\theta \tag{38}$$

where

$$\cos\theta=\frac{v_{e1}(a)}{\sqrt{a^2+v_{e1}^2(a)}} \tag{39}$$

$$\sin\theta=\frac{a}{\sqrt{a^2+v_{e1}(a)}} \tag{40}$$

as also illustrated in Fig. 1. Numerical computation reveals that the $|A_{e1}(a)|^2$ has significant values only for $a\sim 0$ (i.e., $\theta\sim 0$). A specific $|A_e(a)|^2$ distribution is presented in Fig. 2 using polar coordinates. This shows that the excited TE mode inside the planar guide is almost linearly polarized and that the assumptions in writing (3) are valid in the framework of the present analysis.

In Fig. 3 the variation of CE with lateral displacement h (see Fig. 1) is presented for a $w=121.8\ \mu$m interguide

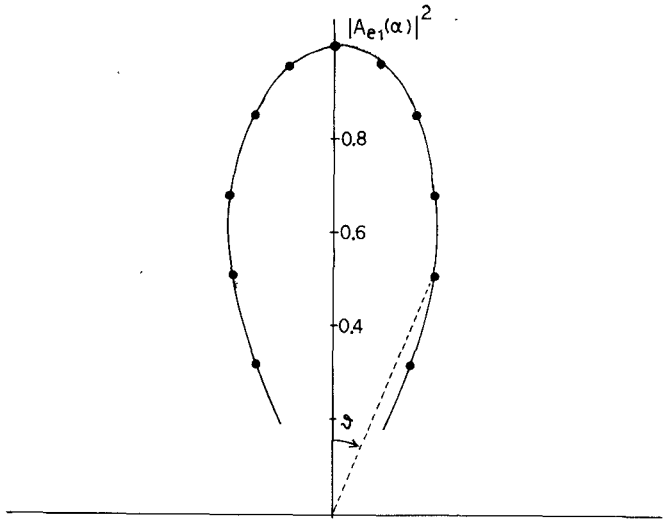

Fig. 2. Dependence of dominant TE planar guide mode amplitude $|A_{e1}(a)|^2$ on propagation direction θ (see Fig. 1 and (39), (40)) for $w = 120$ μm and $h = 0$.

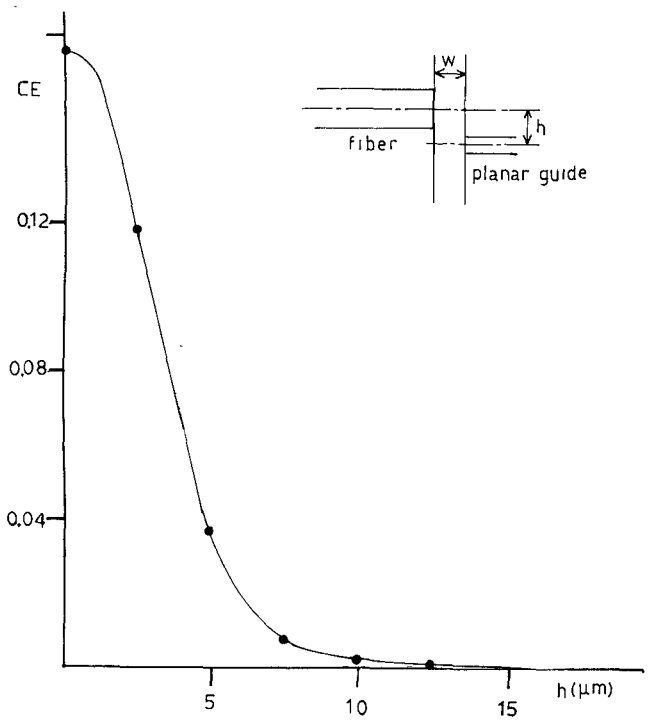

Fig. 3. Variation of coupling efficiency (CE) with the lateral displacement between the two guide axes h (see Fig. 1) for a single-mode fiber with $b = 5$ μm, $n_1 = 1.450$, and $n_2 = 1.454$ and a dielectric planar guide $2d = 1$ μm, $n_1' = 3.40$, and $n_2' = 3.61$ at $\lambda_0 = 1.55$ μm operation wavelength. The interguide distance is $w = 121.8$ μm and $n_0 = 1$.

distance. It is observed that an $h = 5$ μm displacement could reduce the coupling efficiency 6 dB below the peak CE when $h = 0$. The dependence of CE on the interguide distance w is investigated for small displacements around $w = 60$ μm and $w = 120$ μm distances. The expected standing wave patterns are observed in Fig. 4 when the two guide axes coincide (i.e., $h = 0$). The average CE values are approximately equal to 0.15, and it is slightly higher for $w \sim 60$ μm distances. Furthermore, the CE fluctuates

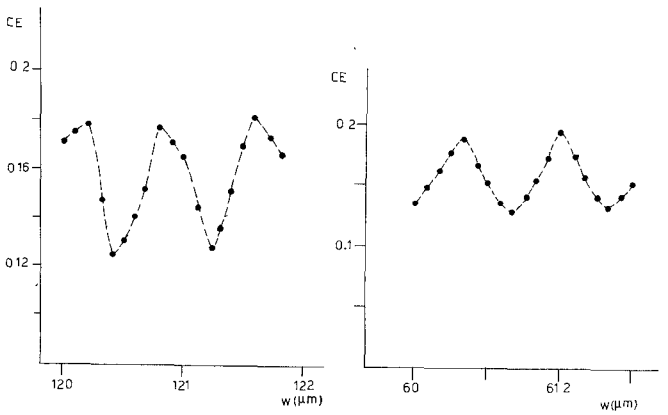

Fig. 4. Dependence of coupling efficiency (CE) on interguide distance w for $h = 0$ and the same set of parameters as in Fig. 3.

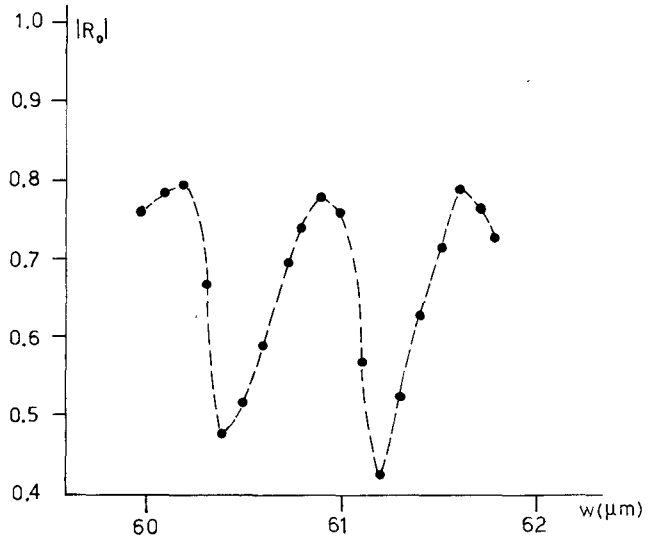

Fig. 5. Variation of $|R_0|$ reflection coefficient of the fiber guide for the same set of parameter values as in Fig. 3 and $h = 0$.

from 0.12 to 0.18 periodically. The period is equal to the free-space wavelength $\lambda_0 = 2\pi/k_0 = 1.55$ μm.

The variation of the reflection coefficient R_0 on the fiber guide has also been computed. In Fig. 5, the variation of $|R_0|$ with interguide distance w is presented. A significant fluctuation (almost 100 percent) is observed in the reflected power inside the fiber guide when the interguide distance w changes by half a wavelength. Comparing Figs. 4 and 5, it is shown that when CE is high R_0 is low, and vice versa.

It is necessary to point out that in practice planar dielectric slab waveguides (i.e., laser diodes) always have finite width (along with y' axis, see Fig. 1). Therefore, the infinite-width planar guide assumed in this paper is an approximation for the fiber–laser diode coupling. Considering the rather large width of laser diodes (~ 20 μm) and the fact that the guided waves inside the planar guide are taken with an arbitrary propagation direction on the $x'y'$ plane, the spillover radiation entering the planar guide for $y \gg \lambda_0$ is expected to be insignificant.

V. Conclusions

The coupling between an abruptly terminated single-mode optical fiber and a dielectric planar waveguide has been analyzed. Weak guidance approximations in both guides are employed to simplify the analysis and to achieve tractability. Furthermore, the same weak guidance conditions are employed to obtain approximate analytical results where only a few numerical integrations are required to obtain numerical results. Computations shows that a coupling efficiency of around 20 percent could be achieved between the two guides under proper alignment. The most critical tolerance seems to be lateral (i.e., h parameter of Fig. 1) displacement of the two guide axes. The fluctuation of the coupling efficiency with the interguide-distance micromovements signifies the critical dependence of laser diode operation on strong externally reflected power levels in optical transmitter systems.

Appendix

A. Single-Mode Fiber Guide Spectrum

Guided Modes:

$$\psi_0(\rho,\varphi)=C_0\begin{cases}\dfrac{K_0(a_0b)}{J_0(a_0b)}J_0(a_0\rho) & \text{for } \rho<b\\ K_0(\gamma\rho) & \text{for } \rho>b\end{cases} \tag{A1}$$

where $a_0=(k_0^2n_2^2-\beta_0^2)^{1/2}$ and $\gamma=(\beta_0^2-k_0^2n_1^2)^{1/2}$. The propagation constant β_0 is obtained by solving the transcendental equation

$$\frac{a_0J_0'(a_0b)}{J_0(a_0b)}=\frac{\gamma K_0'(\gamma b)}{K_0(\gamma b)} \tag{A2}$$

and the normalization constant C_0 of the lowest order mode is

$$C_0=\frac{2J_0^2(a_0b)}{b^2\left(J_0^2(a_0b)K_1^2(\gamma b)+K_0^2(\gamma b)J_1^2(a_0b)\right)} \tag{A3}$$

so that

$$\int_0^{+\infty}\rho\,d\rho\,\psi_0(\rho,\varphi)\psi_0^*(\rho,\varphi)=1$$

is satisfied.

Radiation Modes:

$$\psi_m(\rho,\varphi|q)=\Lambda_m e^{jm\varphi}\begin{cases}\dfrac{J_m(\sigma\rho)}{C_m(q)} & \text{for } p<b\\ \left(J_m(q\rho)+D_m(q)Y_m(q\rho)\right) & \text{for } \rho>b\end{cases} \tag{A4}$$

where $m=0,\pm1,\pm2,\pm3,\cdots,;\ 0<q<+\infty$; and

$$C_m(q)=\frac{\sigma J_m'(\sigma b)Y_m(qb)-J_m(\sigma b)Y_m'(qb)q}{qJ_m'(qb)Y_m(qb)-J_m(\sigma b)Y_m'(qb)q} \tag{A5}$$

$$D_m(q)=\frac{qJ_m(\sigma b)J_m'(qb)-J_m'(\sigma b)J_m(qb)}{J_m'(\sigma b)Y_m(qb)-qJ_m(\sigma b)Y_m'(qb)} \tag{A6}$$

$$\sigma=\left(k_0^2n_2^2-\beta^2\right)^{1/2}\qquad \beta=\left(k_0^2n_1^2-q^2\right)^{1/2}$$

$$\Lambda_m=\left(1+D_m^2\right)^{-1/2}.$$

Orthogonality Relations:

$$\frac{1}{2\pi}\int_{\rho=0}^{+\infty}\rho\,d\rho\int_{\varphi=0}^{2\pi}d\varphi\,\psi_m(\rho,\varphi|q)\psi^*_{m'}(\rho,\varphi|q')=\frac{1}{q}\delta(q-q')\delta'_{mm} \tag{A7}$$

$$\frac{1}{2\pi}\int_{\rho=0}^{+\infty}\rho\,d\rho\int_{\varphi=0}^{2\pi}d\varphi\,\psi_0(\rho,\varphi)\psi^*_{m'}(\rho,\varphi|q)=0. \tag{A8}$$

B. Planar Guide Spectrum

Guided Modes: For even modes,

$$U_{en}(x)=G_{en}\begin{cases}e^{\gamma_e(x+d)} & \text{for } x<-d\\ \dfrac{\cos(K_ex)}{\cos(K_ed)} & \text{for } -d\leqslant x\leqslant d\\ e^{-\gamma_e(x-d)} & \text{for } x>d\end{cases}$$

$$G_{en}=\left(\gamma_e^{-1}+\gamma_e/K_e^2+d/\cos^2(K_ed)\right)^{-1/2}.$$

For odd modes,

$$U_{0n}(x)=G_{0n}\begin{cases}-e^{\gamma_e(x+d)} & \text{for } x<-d\\ \dfrac{\sin(K_0x)}{\sin(K_0d)} & \text{for } -d\leqslant x\leqslant d\\ e^{-\gamma_0(x-d)} & \text{for } x>d\end{cases}$$

$$G_{0n}=\left(\gamma_0^{-1}+\gamma_0/K_0^2+d/\sin^2(K_0d)\right)^{-1/2}. \tag{A9}$$

Transcendental equations:

$$\gamma_e=K_e\tan(K_ed)\qquad K_0=-\gamma_0\tan(K_0d)$$

$$\gamma_e=\left(a^2+v^2-k_0^2n_1^2\right)^{1/2}$$

$$K_e=\left(k_0^2n_2^2-a^2-v_e^2\right)^{1/2}.$$

Orthogonality relations:

$$\int_{-\infty}^{+\infty}u_{en}(x)u_{em}(x)\,dx=\delta_{nm} \tag{A10}$$

$$\int_{-\infty}^{+\infty}dx\,u_{en}(x)u_{on}(x)=0. \tag{A11}$$

Radiation Modes: For even modes,

$$\varphi_e(x,p)=\frac{1}{\sqrt{\pi}}\begin{cases}\cos\left(p(x+d)-\chi_\rho(p)\right) & \text{for } x<-d\\ \dfrac{1}{C_e(p)}\dfrac{\cos(\sigma x)}{\cos(\sigma d)} & \text{for } -d\leqslant x\leqslant d\\ \cos\left(p(x-d)+\chi_e(p)\right) & \text{for } x>d.\end{cases}$$

For odd modes,

$$\varphi_0(x,p)=\frac{1}{\sqrt{\pi}}\begin{cases}\sin\left(p(x+d)-\chi_0(p)\right) & \text{for } x-d\\ \dfrac{1}{C_0(p)}\dfrac{\sin(\sigma x)}{\sin(\sigma d)} & \text{for } -d<x<d\\ \sin\left(p(x-d)+\chi_0(p)\right) & \text{for } x>d\end{cases}$$

$$\sigma=\sqrt{k_0^2(n_2^2-n_1^2)+p^2} \tag{A12}$$

$$\chi_e(p)=\tan^{-1}\left(\frac{\sigma}{p}\tan(\sigma d)\right)$$

$$\chi_0(p)=\tan^{-1}\left(\frac{p}{\sigma}\tan(\sigma d)\right)$$

$$C_e(p)=\sqrt{1+\frac{\sigma^2}{p^2}\tan^2(\sigma d)}$$

$$C_0(p)=\sqrt{1+\frac{\sigma^2}{p^2}\frac{1}{\tan^2(\sigma d)}}\,.$$

Orthogonality relations:

$$\int_0^{+\infty}\varphi_e(x,p)\varphi_e(x',p)\,dx=\delta(p-p') \tag{A13}$$

$$\int_0^{+\infty}\varphi_e(x,p)\varphi_0(x,p')\,dx=0. \tag{A14}$$

C. $I_u(\lambda)$ Integral of (33)

$$I_u(\lambda)=G_{e1}\left[\frac{\cos\left(\sqrt{\lambda^2-a^2}\,d\right)}{\sqrt{\lambda^2-a^2}}\frac{1}{2}\left[\frac{\sin\left(K_e+\sqrt{\lambda^2-a^2}\right)d)}{K_e+\sqrt{\lambda^2-a^2}}+\frac{\sin\left(\left(K_e-\sqrt{\lambda^2-a^2}\right)d\right)}{K_e-\sqrt{\lambda^2-a^2}}\right]\right.$$

$$\left.=\frac{\sqrt{\lambda^2-a^2}\sin\left(\sqrt{\lambda^2-a^2}\,d\right)-\gamma_n\cos\left(\sqrt{\lambda^2-a^2}\,d\right)}{\gamma_n^2+\lambda^2-a^2}\right]. \tag{A15}$$

References

[1] I. Garett and J. E. Midwinter, "Optical communication systems," in *Optical Fibre Communications*, M. J. Howes and D. V. Morgan, Eds. New York: Wiley, 1980, pp. 251–299.

[2] P. A. Kirby, "Semiconductor laser sources for optical communication," *Radio Electron Eng.*, vol. 51, pp. 363–376, 1981.

[3] R. Itoh, "Hybrid laser-to-fiber coupler with a cylindrical lens," *Appl. Opt.*, vol. 16, pp. 1966–1970, July 1977.

[4] D. Kato, "Light coupling from a stripe-geometry GaAs diode laser into an optical fiber with spherical end," *J. Appl. Phys.*, vol. 44, pp. 2756–2758, 1973.

[5] C. A. Brackett, "On the efficiency of coupling light from stripe-geometry GaAs lasers into multimode optical fibers," *J. Appl. Phys.*, vol. 45, pp. 2636–2637, 1974.

[6] K. Kawano, H. Miyazawa, and O. Mitomi, "New calculations for coupling laser diode to multimode fiber," *J. Lightwave Technol.*, vol. LT-4, pp. 368–374, 1986.

[7] C. N. Capsalis, J. G. Fikioris, and N. K. Uzunoglu, "Scattering from an abruptly terminated dielectric-slab waveguide," *J. Lightwave Technol.*, vol. LT-3, pp. 408–415, 1985.

[8] J. Senior, *Optical Fiber Communications: Principles and Practises*. London: Prentice-Hall, 1985.

[9] A. Snyder and J. D. Love, *Optical Waveguide Theory*. New York. Chapman and Hall, 1983, chs. 25 and 32.

[10] H. Kogelnik, "Theory of dielectric waveguides," in *Integrated Optics* (Topics in Applied Physics, vol. 7), T. Tamir, Ed. New York: Springer-Verlag, 1982, pp. 13–81.

[11] H. G. Unger, *Planar Optical Waveguides and Fibres*. Oxford: Clarendon Press, 1977, ch. 4.

[12] D. S. Jones, *Theory of Electromagnetism*. Oxford: Pergamon Press, 1964.

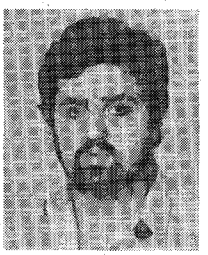

Christos N. Capsalis was born in Nafplion, Greece, on September 25, 1956. He received the Diploma of E.E. and M.E. from the National Technical University of Athens (NTUA) in 1979 and the bachelor's degree in economics from the University of Athens in 1983. He also received the doctor's degree in electrical engineering from NTUA in 1985.

Since January 1982, he has been a Research Associate in the Department of Electrical Engineering at NTUA. In November 1986 he was elected Lecturer at NTUA. His main research interests are in the electromagnetic field area, with emphasis on scattering and propagation at millimeter and optical wavelengths.

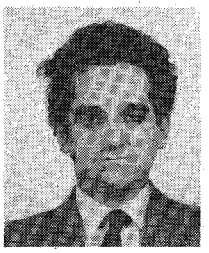

Nikolaos K. Uzunoglu (M'82) received the B.Sc. degree in electronics engineering from the Istanbul Technical University, Turkey, in 1973. He obtained the M.Sc. and Ph.D. degrees from the University of Essex, England, in 1974 and 1976, respectively.

He worked for the Hellenic Navy Research and Technology Development Office from 1977 to 1984. During this period, he also worked on a part-time basis at the National Technical University on electromagnetic theory. In 1984, he was electged Associate Professor at the National Technical University of Athens, the position that he holds presently. His research interestes are microwave applications, fiber optics, and electromagnetic theory.